Physics of Fluids

RESEARCH ARTICLE | MARCH 21 2024

How do various forces affect pressure waves in bubbly flows?

Shuya Arai (新井秀弥) ; Tetsuya Kanagawa (金川哲也)

Physics of Fluids 36, 033352 (2024)
https://doi.org/10.1063/5.0187533

How do various forces affect pressure waves in bubbly flows?

Cite as: Phys. Fluids 36, 033352 (2024); doi: 10.1063/5.0187533
Submitted: 14 November 2023 · Accepted: 22 December 2023 ·
Published Online: 21 March 2024

Shuya Arai (新井秀弥),[1] and Tetsuya Kanagawa (金川哲也)[2,a)]

AFFILIATIONS

[1]Department of Engineering Mechanics and Energy, Degree Programs in Systems and Information Engineering, University of Tsukuba, Tsukuba 305-8573, Japan
[2]Department of Engineering Mechanics and Energy, Institute of Systems and Information Engineering, University of Tsukuba, Tsukuba 305-8573, Japan

[a)]Author to whom correspondence should be addressed: kanagawa.tetsuya.fu@u.tsukuba.ac.jp

ABSTRACT

This study investigated the weakly nonlinear propagation of pressure waves in compressible, flowing water with spherical microbubbles, considering various forces. Previous theoretical studies on nonlinear pressure waves in bubbly flows did not consider the forces acting on the bubbles, although the validity of ignoring these forces has not been demonstrated. We focused on every possible force such as drag, gravity, buoyancy, and Bjerknes (acoustic radiation) forces acting on bubbles and studied their effects on pressure waves in a one-dimensional setting. Using a singular perturbation method, the Korteweg–de Vries–Burgers equation describing wave propagation was derived. The following results were obtained: (i) Bjerknes force on the bubbles enhanced the nonlinearity, dissipation, and dispersion of the waves; (ii) Drag, gravity, and buoyancy forces acting on the bubbles increased wave dissipation; (iii) Thermal conduction had the most substantial dissipation effect, followed by acoustic radiation, drag, buoyancy, and gravity. We confirmed that the dissipation due to forces on gas bubbles was quantitatively minor.

I. INTRODUCTION

A pressure wave in a bubbly flow evolves into a shock wave[1–3] or stable wave [sometimes referred to as (acoustic) soliton]; these waves exhibit extremely different properties. A shock wave and an acoustic soliton evolve based on the competition between nonlinearity and dissipation and that between nonlinearity and dispersion, respectively. To predict the evolution waveform, the relative strengths of three properties, i.e., nonlinearity, dissipation, and dispersion, must be clarified. Many studies have been conducted on pressure waves in bubbly flows by experiments[4–11] or numerical simulations.[12–26] However, three properties mentioned above are difficult to obtain quantitatively by experiments or numerical analysis alone; nonlinear wave equations based on theoretical analysis[27,28] is an effective method for clarifying these properties. Moreover, the advantage of theoretical analysis is that the factors of wave attenuation can be considered separately and evaluated quantitatively. The weakly nonlinear (i.e., finite but small amplitude)[29] propagation of pressure waves in bubble flows is described by nonlinear wave equations,[30,31] among which the Korteweg–de Vries–Burgers (KdVB) equation[32–35] for low-frequency long waves is popular. In particular, it is shown that the waveform obtained from the KdVB equation agrees with the experimental outcome.[36] As the KdVB equation is expressed as a linear combination of nonlinear, dissipation, and dispersion terms, estimating the functions and values of these three terms leads to the elucidation of the evolution waveform.

Various forces act on the gas bubbles, such as drag,[37–43] lift,[44–46] gravity,[47,48] buoyancy,[48,49] virtual mass force,[50] and Bjerknes (acoustic radiation) force.[51–58] However, the relationship between the forces acting on bubbles and waves in bubbly flows has not been clarified. Previous theoretical studies[32–36] on nonlinear pressure waves in bubbly flows did not incorporate forces acting on the bubble, although the validity of ignoring these forces has not been demonstrated. This may be because of the preconception that the forces (non-oscillations) do not affect the waves (oscillations). Recently, our previous studies[59–63] introduced the drag force into the KdVB equation and showed that the drag force increased wave dissipation. However, the effects of gravity, buoyancy, and Bjerknes forces on waves have not been discussed. In particular, the primary Bjerknes force is the acoustic radiation pressure that is always applied to oscillation bubbles in the propagation of ultrasonic waves.[64–69] Therefore, this cannot be ignored when dealing with wave theory. Consequently, this study aimed to elucidate the effects of various forces, such as gravity, buoyancy, and Bjerknes forces on pressure waves in bubbly flows by deriving the KdVB equation.

The remainder of this paper is configured as follows. In Sec. II, we introduce the basic equations of the two-fluid model, including drag, gravity, buoyancy, and Bjerknes forces. In Sec. III, we derive the KdVB equation and show that the gravity and buoyancy forces, such as the drag force, increase the dissipation of the waves, whereas the Bjerknes force increases the nonlinearity, dissipation, and dispersion of the waves. We clarified that the dissipation effect of thermal conduction is the largest, followed by those of acoustic radiation. drag, buoyancy, and gravity, based on numerical analysis. Finally, Sec. IV concludes the paper. Because this study clarifies that the attenuation of waves owing to the forces acting on gas bubbles is quantitatively small, this study is the first demonstration of the validity of ignoring forces for pressure wave propagation in bubbly flows.

II. PROBLEM FORMULATION

A. Problem statement

We conduct a theoretical investigation of the weakly nonlinear (i.e., finite but small amplitude) propagation of plane (one-dimensional) progressive pressure waves in flowing compressible water uniformly containing numerous small spherical gas bubbles under various forces, as shown in Fig. 1; i.e., drag, gravity, buoyancy, and Bjerknes (acoustic radiation) forces [see (7)–(10) below] are incorporated.

On the other hand, we shall simply the problem based on the following assumptions: (i) The primary Bjerknes force is accounted for, while the secondary Bjerknes force[70–74] is excluded from consideration; (ii) To simplify the model, direct interactions between bubbles, gas-phase viscosity, Reynolds stress, and phase change and mass transport across the bubble–liquid interface are neglected; (iii) The motion of bubbles is assumed to be spherically symmetric; (iv) Bubbles remain stable, without coalescing, breaking, becoming extinct, or forming anew; (v) The liquid temperature is constant; (vi) In the initial state, both gas and liquid phases flow at constant velocities.

B. Basic equations

To introduce various forces into the interfacial momentum transport, we apply the conservation equations of mass and momentum for the gas and liquid phases based on a two-fluid model[75,76] as follows:

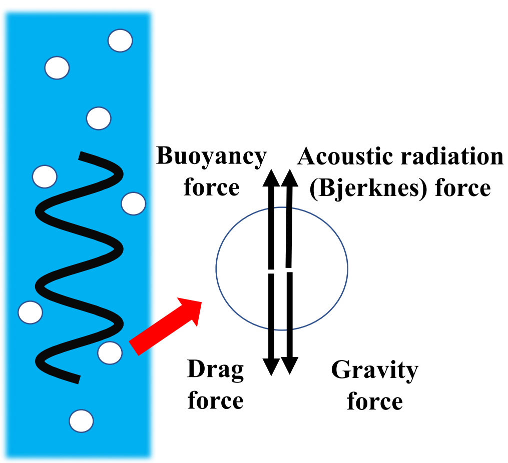

FIG. 1. Schematic illustration of one-dimensional propagation of pressure waves in bubbly flows; drag, gravity, buoyancy, and acoustic radiation (primary Bjerknes) forces acting on each bubble. The direction of these forces is an example.

$$\frac{\partial}{\partial t^*}(\alpha\rho_{\rm G}^*) + \frac{\partial}{\partial x^*}(\alpha\rho_{\rm G}^* u_{\rm G}^*) = 0, \tag{1}$$

$$\frac{\partial}{\partial t^*}\left[(1-\alpha)\rho_{\rm L}^*\right] + \frac{\partial}{\partial x^*}\left[(1-\alpha)\rho_{\rm L}^* u_{\rm L}^*\right] = 0, \tag{2}$$

$$\frac{\partial}{\partial t^*}(\alpha\rho_{\rm G}^* u_{\rm G}^*) + \frac{\partial}{\partial x^*}(\alpha\rho_{\rm G}^* u_{\rm G}^{*2}) + \alpha\frac{\partial p_{\rm G}^*}{\partial x^*} + 2\mu_{\rm L}^*\frac{\partial u_{\rm L}^*}{\partial x^*}\frac{\partial \alpha}{\partial x^*} = F_{\rm vm}^* + F_{\rm dr}^* + F_{\rm bje}^* + F_{\rm buo}^* + F_{\rm gr,G}^*, \tag{3}$$

$$\frac{\partial}{\partial t^*}\left[(1-\alpha)\rho_{\rm L}^* u_{\rm L}^*\right] + \frac{\partial}{\partial x^*}\left[(1-\alpha)\rho_{\rm L}^* u_{\rm L}^{*2}\right] + (1-\alpha)\frac{\partial p_{\rm L}^*}{\partial x^*} + P^*\frac{\partial \alpha}{\partial x^*} - 2\mu_{\rm L}^*(1-\alpha)\frac{\partial^2 u_{\rm L}^*}{\partial x^{*2}} = -F_{\rm vm}^* - F_{\rm dr}^* - F_{\rm bje}^* - F_{\rm buo}^* + F_{\rm gr,L}^*, \tag{4}$$

where t^* is the time, x^* is the space coordinate normal to the wavefront, α is the void fraction ($0 < \alpha < 1$), μ^* is the viscosity, ρ^* is the density, u^* is the velocity, p^* is the pressure, and P^* is the liquid pressure averaged over the bubble–liquid interface.[76] The superscript $*$ denotes a dimensional quantity, and the subscripts G and L denote the volume-averaged variables in the gas and liquid phases, respectively.

As interfacial momentum transport terms, the following model of virtual mass force[50] is introduced:

$$F_{\rm vm}^* = -\beta_1\alpha\rho_{\rm L}^*\left(\frac{{\rm D_G}u_{\rm G}^*}{{\rm D}t^*} - \frac{{\rm D_L}u_{\rm L}^*}{{\rm D}t^*}\right) - \beta_2\rho_{\rm L}^*(u_{\rm G}^* - u_{\rm L}^*)\frac{{\rm D_G}\alpha}{{\rm D}t^*} - \beta_3\alpha(u_{\rm G}^* - u_{\rm L}^*)\frac{{\rm D_G}\rho_{\rm L}^*}{{\rm D}t^*}, \tag{5}$$

where β_1, β_2, and β_3 are constants that can be set as 1/2 for a spherical bubble. The Lagrange derivatives ${\rm D_G}/{\rm D}t^*$ and ${\rm D_L}/{\rm D}t^*$ are defined as follows:

$$\frac{\rm D_G}{{\rm D}t^*} = \frac{\partial}{\partial t^*} + u_{\rm G}^*\frac{\partial}{\partial x^*}, \quad \frac{\rm D_L}{{\rm D}t^*} = \frac{\partial}{\partial t^*} + u_{\rm L}^*\frac{\partial}{\partial x^*}. \tag{6}$$

Furthermore, we introduce a model for the drag force term $F_{\rm dr}^*$ for spherical bubbles,[59]

$$F_{\rm dr}^* = -\frac{3}{8R^*}\alpha C_{\rm D}\rho_{\rm L}^*(u_{\rm G}^* - u_{\rm L}^*)|u_{\rm G}^* - u_{\rm L}^*|, \tag{7}$$

where R^* is a representative bubble radius and $C_{\rm D}$ is the drag coefficient for a single spherical bubble. We also introduce the gravity, buoyancy, and (primary) Bjerknes forces,[48,49]

$$F_{\rm gr,G}^* = -\alpha\rho_{\rm G}^* g^*, \quad F_{\rm gr,L}^* = -(1-\alpha)\rho_{\rm L}^* g^*, \tag{8}$$

$$F_{\rm buo}^* = \alpha\rho_{\rm L}^* g^*, \tag{9}$$

$$F_{\rm bje}^* = -B\alpha\frac{\partial p_{\rm L}^*}{\partial x^*}, \tag{10}$$

where g^* is the acceleration of gravity and B is a constant. Note that gravity acting on each phase is considered. We will focus on the presence of B to verify the effect of the Bjerknes force, i.e., $B = 0$ and $B = 1$ correspond to the cases of without and with the Bjerknes force, respectively.

We employ the equation of motion for the bubbles, formulated as a linear combination of their volumetric oscillations[77] and translation movements.[78–80] This approach integrates the dynamics of bubble oscillation and translation to comprehensively describe their motion:

$$\left(1 - \frac{1}{c_{\rm L0}^*}\frac{{\rm D_G}R^*}{{\rm D}t^*}\right)R^*\frac{{\rm D_G^2}R^*}{{\rm D}t^{*2}} + \frac{3}{2}\left(1 - \frac{1}{3c_{\rm L0}^*}\frac{{\rm D_G}R^*}{{\rm D}t^*}\right)\left(\frac{{\rm D_G}R^*}{{\rm D}t^*}\right)^2 = \left(1 + \frac{1}{c_{\rm L0}^*}\frac{{\rm D_G}R^*}{{\rm D}t^*}\right)\frac{P^*}{\rho_{\rm L0}^*} + \frac{R^*}{\rho_{\rm L0}^* c_{\rm L0}^*}\frac{\rm D_G}{{\rm D}t^*}(p_{\rm L}^* + P^*) + \frac{(u_{\rm G}^* - u_{\rm L}^*)^2}{4}, \tag{11}$$

where c^*_{L0} is the initial speed of sound in pure water.

In this study, the energy equation[81] for thermal conduction at the bubble–liquid interface is introduced to account for the thermal effects within the bubble:

$$\frac{D_G p^*_G}{Dt^*} = \frac{3}{R^*}\left[(\kappa-1)\lambda^*_G \frac{\partial T^*_G}{\partial r^*}\bigg|_{r^*=R^*} - \kappa p^*_G \frac{D_G R^*}{Dt^*}\right], \tag{12}$$

where T^*_G is the gas temperature, κ is the ratio of specific heats, r^* is the radial distance from the center of the bubble, and λ^*_G is the thermal conductivity of the gas inside the bubble. Prosperetti[81] did not use a temperature-gradient model. However, certain models for the temperature-gradient as the first term on the right-hand side of (12) were proposed. This study uses the model proposed by Sugiyama *et al.*,[82]

$$\frac{\partial T^*_G}{\partial r^*}\bigg|_{r^*=R^*} = \frac{\mathrm{Re}(\widetilde{L^*_p})(T^*_{G0}-T^*_G)}{|\widetilde{L^*_p}|^2} + \frac{\mathrm{Im}(\widetilde{L^*_p})}{\omega^*_B|\widetilde{L^*_p}|^2}\frac{D_G T^*_G}{Dt^*}, \tag{13}$$

where Re and Im denote the real and imaginary parts, respectively. The physical quantities in the initial state are denoted by the subscript 0 and are constants. Certain symbols are defined as follows:[82]

$$\omega^*_B = \sqrt{\frac{3\gamma_e(p^*_{L0}+2\sigma^*/R^*_0)-2\sigma^*/R^*_0}{\rho^*_{L0}R^{*2}_0} - \left(\frac{2\mu^*_{e0}}{\rho^*_{L0}R^{*2}_0}\right)^2}, \tag{14}$$

$$\gamma_e = \mathrm{Re}\left(\frac{\Gamma_N}{3}\right), \tag{15}$$

$$\mu^*_{e0} = \mu^*_L + \mathrm{Im}\left(\frac{p^*_{G0}\Gamma_N}{4\omega^*_B}\right), \tag{16}$$

$$\Gamma_N = \frac{3\alpha_N^2\kappa}{\alpha_N^2 + 3(\kappa-1)(\alpha_N\coth\alpha_N - 1)}, \tag{17}$$

$$\alpha_N = \sqrt{\frac{\kappa\omega^*_B p^*_{G0}R^{*2}_0}{2(\kappa-1)T^*_{G0}\lambda^*_G}}(1+\mathrm{i}), \tag{18}$$

$$\widetilde{L^*_p} = \frac{R^*_0(\alpha_N^2 - 3\alpha_N\coth\alpha_N + 3)}{\alpha_N^2(\alpha_N\coth\alpha_N - 1)}, \tag{19}$$

where ω^*_B is the eigenfrequency of a single bubble, γ_e is the effective polytropic exponent, μ^*_{e0} is the initial effective viscosity, σ^* is the surface tension, i denotes an imaginary unit, and Γ_N, α_N, and $\widetilde{L^*_p}$ are complex numbers.

To close the set of (1)–(4), (11), and (12), the equation of state for an ideal gas, the Tait equation of state for liquid, the mass conservation law of gas inside the bubbles, and the balance of normal stresses across the bubble–liquid interface, are introduced as follows:

$$\frac{p^*_G}{p^*_{G0}} = \frac{\rho^*_G}{\rho^*_{G0}}\frac{T^*_G}{T^*_{G0}}, \tag{20}$$

$$p^*_L = p^*_{L0} + \frac{\rho^*_{L0}c^{*2}_{L0}}{n}\left[\left(\frac{\rho^*_L}{\rho^*_{L0}}\right)^n - 1\right], \tag{21}$$

$$\frac{\rho^*_G}{\rho^*_{G0}} = \left(\frac{R^*_0}{R^*}\right)^3, \tag{22}$$

$$p^*_G - (p^*_L + P^*) = \frac{2\sigma^*}{R^*} + \frac{4\mu^*_L}{R^*}\frac{D_G R^*}{Dt^*}, \tag{23}$$

where n is a material constant (e.g., $n = 7.15$ for water).

C. Analysis on multiple scales

Using the method of multiple scales,[31] we introduce four scales as extended independent variables. This approach is based on the assumption of a finite but small nondimensional wave amplitude, denoted as ϵ ($\ll 1$):

$$t_0 = t, \quad t_1 = \epsilon t; \quad x_0 = x, \quad x_1 = \epsilon x, \tag{24}$$

where the nondimensional independent variables are defined by $t = t^*/T^*$ and $x = x^*/L^*$; T^* is a typical period and L^* is a typical wavelength. Here, the subscripts 0 and 1 correspond to the near and far fields,[31] e.g., t_0 is the nondimensional time for the near field. Note that the difference between the constant is denoted by subscript 0 and near field by 0.

The dependent variables are then nondimensionalized and expanded in the power series of ϵ, as follows:

$$R^*/R^*_0 = 1 + \epsilon R_1 + \epsilon^2 R_2 + O(\epsilon^3), \tag{25}$$

$$u^*_G/U^* = u_{G0} + \epsilon u_{G1} + \epsilon^2 u_{G2} + O(\epsilon^3), \tag{26}$$

$$u^*_L/U^* = u_{L0} + \epsilon u_{L1} + \epsilon^2 u_{L2} + O(\epsilon^3), \tag{27}$$

$$\alpha/\alpha_0 = 1 + \epsilon\alpha_1 + \epsilon^2\alpha_2 + O(\epsilon^3), \tag{28}$$

$$\rho^*_L/\rho^*_{L0} = 1 + \epsilon^2\rho_{L1} + O(\epsilon^3), \tag{29}$$

$$p^*_L/(\rho^*_{L0}U^{*2}) = p_{L0} + \epsilon p_{L1} + \epsilon^2 p_{L2} + O(\epsilon^3), \tag{30}$$

$$T^*_G/T^*_{G0} = 1 + \epsilon T_{G1} + \epsilon^2 T_{G2} + O(\epsilon^3), \tag{31}$$

where $U^*(\equiv L^*/T^*)$ is the typical propagation speed, and the initial nondimensional pressures p_{G0} and p_{L0} are defined as $p_{G0} \equiv p^*_{G0}/(\rho^*_{L0}U^{*2}) \equiv O(1)$ and $p_{L0} \equiv p^*_{L0}/(\rho^*_{L0}U^{*2}) \equiv O(1)$. Further, the ratio of the initial densities of the gas and the liquid phases is sufficiently small.

By using nondimensional ratios based on ϵ, the low-frequency long wave is described by

$$\frac{U^*}{c^*_{L0}} \equiv O(\sqrt{\epsilon}) \equiv V\sqrt{\epsilon}, \tag{32}$$

$$\frac{R^*_0}{L^*} \equiv O(\sqrt{\epsilon}) \equiv \Delta\sqrt{\epsilon}, \tag{33}$$

$$\frac{\omega^*}{\omega^*_B} \equiv \frac{1}{T^*\omega^*_B} \equiv O(\sqrt{\epsilon}) \equiv \Omega\sqrt{\epsilon}, \tag{34}$$

where V, Δ, and Ω are the constants of $O(1)$. Equations (32)–(34) correspond to the present acoustic properties of bubbly flows; i.e., the speed of sound within these flows is significantly lower compared to that in pure water, the initial bubble radius is markedly smaller than the typical wavelength observed in such environments, and the incident frequency of waves within bubbly flows is substantially lower than the eigenfrequency of individual bubbles.

We determine the sizes of the nondimensional numbers for the thermal effect:[61,63]

$$\begin{aligned} \frac{3(\kappa-1)\lambda^*_G}{p^*_{G0}\omega^* R^*_0}\frac{\mathrm{Re}(\widetilde{L^*_p})T^*_{G0}}{|\widetilde{L^*_p}|^2} &= \zeta_{STM1}\epsilon, \\ \frac{3(\kappa-1)\lambda^*_G}{p^*_{G0}\omega^* R^*_0}\frac{\omega^*\mathrm{Im}(\widetilde{L^*_p})T^*_{G0}}{\omega^*_B|\widetilde{L^*_p}|^2} &= \zeta_{STM2}\epsilon^2. \end{aligned} \tag{35}$$

The nondimensionalization of the acceleration owing to gravity g^* is

$$\frac{T^* g^*}{U^*} = g\epsilon, \tag{36}$$

where g is a constant of $O(1)$. The nondimensionalization of the liquid viscosity μ_L^* is defined by

$$\frac{\mu_L^*}{\rho_{L0}^* U^* L^*} \equiv O(\epsilon^2) \equiv \mu_L \epsilon^2, \tag{37}$$

where μ_L is a constant of $O(1)$. The drag coefficient C_D is defined by

$$C_D \equiv \frac{A\mu_L^*}{|u_G^* - u_L^*|\rho_L^* 2R^*}, \tag{38}$$

where A is a constant (e.g., $A = 16$), and C_D depends on the Reynolds number Re ($C_D = A/\text{Re}$).[83]

III. RESULTS

A. Linear propagation at near field

By substituting (24)–(38) into (1)–(4), (11), and (12), we obtain a set of linear equations using (20)–(23) from the leading-order approximation:

$$\frac{D\alpha_1}{Dt_0} - 3\frac{DR_1}{Dt_0} + \frac{\partial u_{G1}}{\partial x_0} = 0, \tag{39}$$

$$\alpha_0 \frac{D\alpha_1}{Dt_0} - (1-\alpha_0)\frac{\partial u_{L1}}{\partial x_0} = 0, \tag{40}$$

$$\beta_1\left(\frac{Du_{G1}}{Dt_0} - \frac{Du_{L1}}{Dt_0}\right) - 3p_{G0}\frac{\partial R_1}{\partial x_0} + p_{G0}\frac{\partial T_{G1}}{\partial x_0} + B\frac{\partial p_{L1}}{\partial x_0} = 0, \tag{41}$$

$$(1-\alpha_0)\frac{Du_{L1}}{Dt_0} - \alpha_0\beta_1\left(\frac{Du_{G1}}{Dt_0} - \frac{Du_{L1}}{Dt_0}\right) - \alpha_0 u_0 \frac{D\alpha_1}{Dt_0} + u_0(1-\alpha_0)\frac{\partial u_{L1}}{\partial x_0} + (1-\alpha_0)\frac{\partial p_{L1}}{\partial x_0} - \alpha_0 B\frac{\partial p_{L1}}{\partial x_0} = 0, \tag{42}$$

$$\left[3(\gamma_e - 1)p_{G0} - \frac{\Delta^2}{\Omega^2}\right]R_1 + p_{G0}T_{G1} - p_{L1} = 0, \tag{43}$$

$$\frac{DT_{G1}}{Dt_0} + 3(\kappa - 1)\frac{DR_1}{Dt_0} = 0. \tag{44}$$

Although gravitational and buoyancy forces do not appear here, the effect of the Bjerknes force ($F_{bje}^* = -B\alpha\partial p_L^*/\partial x^*$) is described by the last term on the left side of (41) and (42).

Combining (39)–(44) results in a linear wave equation for the first-order variation in the bubble radius R_1,

$$\frac{D^2 R_1}{Dt_0^2} - v_p^2 \frac{\partial^2 R_1}{\partial x_0^2} = 0, \tag{45}$$

where v_p is the phase velocity expressed as

$$v_p = \sqrt{\frac{\alpha_0\kappa(1-\alpha_0+\beta_1) - (\beta_1+\alpha_0 B)(1-\alpha_0)(\gamma_e-\kappa)}{\alpha_0\beta_1(1-\alpha_0)}p_{G0} + \frac{\beta_1+\alpha_0 B}{3\alpha_0\beta_1}\frac{\Delta^2}{\Omega^2}}. \tag{46}$$

The linear Lagrange derivative D/Dt_0 is defined as

$$\frac{D}{Dt_0} = \frac{\partial}{\partial t_0} + u_0\frac{\partial}{\partial x_0}. \tag{47}$$

For simplicity, the initial velocities of both phases are assumed to be the same ($u_{G0} = u_{L0} \equiv u_0$). However, the perturbations of the velocities are not the same ($u_{G1} \neq u_{L1}$). Setting $v_p = 1$ yields the explicit form of U^* as

$$U^* = \sqrt{\frac{\alpha_0\kappa(1-\alpha_0+\beta_1) - (\beta_1+\alpha_0 B)(1-\alpha_0)(\gamma_e-\kappa)}{\alpha_0\beta_1(1-\alpha_0)}\frac{p_{G0}^*}{\rho_{L0}^*} + \frac{\beta_1+\alpha_0 B}{3\alpha_0\beta_1}R_0^{*2}\omega_B^{*2}}. \tag{48}$$

Value of the typical propagation speed U^* is increased by considering the Bjerknes force as shown in Table I.

By focusing on the right-running wave (i.e., by introducing the moving coordinates $\varphi_0 = x_0 - v_p t_0$), α_1, u_{G1}, u_{L1}, p_{L1}, and T_{G1} are expressed in terms of R_1.

$$\alpha_1 = s_1 R_1, \quad u_{G1} = s_2 R_1, \quad u_{L1} = s_3 R_1, \quad p_{L1} = s_4 R_1, \quad T_{G1} = s_5 R_1 \tag{49}$$

with

$$s_1 = \frac{(1-\alpha_0)}{\alpha_0(1-\alpha_0+\beta_1)}\left[3\alpha_0\beta_1 - \frac{(1-\alpha_0-\alpha_0 B)s_4}{v_p^2}\right], \quad s_2 = v_p(s_1 - 3),$$
$$s_3 = -v_p\frac{\alpha_0}{1-\alpha_0}s_1, \quad s_4 = 3p_{G0}(\gamma_e - \kappa) - \frac{\Delta^2}{\Omega^2}, \quad s_5 = -3(\kappa - 1). \tag{50}$$

TABLE I. Value of the typical propagation speed U^*.

R_0^*	α_0	$U^*\|_{B=0}$ [m/s]	$(U^*\|_{B=1} - U^*\|_{B=0})/U^*\|_{B=0}$
5 mm	0.0001 (0.01%)	1.2×10^3	0.010
	0.001 (0.1%)	3.8×10^2	0.10
	0.01 (1%)	1.2×10^2	0.97
500 μm	0.0001 (0.01%)	1.2×10^3	0.010
	0.001 (0.1%)	3.8×10^2	0.10
	0.01 (1%)	1.2×10^2	0.97
50 μm	0.0001 (0.01%)	1.2×10^3	0.010
	0.001 (0.1%)	3.8×10^2	0.10
	0.01 (1%)	1.2×10^2	0.97

Note that s_1, s_2, and s_3 change due to the effects of the Bjerknes force, whereas s_4 and s_5 do not change.

B. Nonlinear propagation at far field

As in the case of $O(\epsilon)$, the following set of inhomogeneous equations for $O(\epsilon^2)$ is derived:

$$\frac{\mathrm{D}\alpha_2}{\mathrm{D}t_0} - 3\frac{\mathrm{D}R_2}{\mathrm{D}t_0} + \frac{\partial u_{\mathrm{G2}}}{\partial x_0} = K_1, \tag{51}$$

$$\alpha_0 \frac{\mathrm{D}\alpha_2}{\mathrm{D}t_0} - (1-\alpha_0)\frac{\partial u_{\mathrm{L2}}}{\partial x_0} = K_2, \tag{52}$$

$$\beta_1\left(\frac{\mathrm{D}u_{\mathrm{G2}}}{\mathrm{D}t_0} - \frac{\mathrm{D}u_{\mathrm{L2}}}{\mathrm{D}t_0}\right) - 3p_{\mathrm{G0}}\frac{\partial R_2}{\partial x_0} + p_{\mathrm{G0}}\frac{\partial T_{\mathrm{G2}}}{\partial x_0} + B\frac{\partial p_{\mathrm{L2}}}{\partial x_0} = K_3, \tag{53}$$

$$(1-\alpha_0)\frac{\mathrm{D}u_{\mathrm{L2}}}{\mathrm{D}t_0} - \alpha_0\beta_1\left(\frac{\mathrm{D}u_{\mathrm{G2}}}{\mathrm{D}t_0} - \frac{\mathrm{D}u_{\mathrm{L2}}}{\mathrm{D}t_0}\right) - \alpha_0 u_0\frac{\mathrm{D}\alpha_2}{\mathrm{D}t_0} + u_0(1-\alpha_0)\frac{\partial u_{\mathrm{L2}}}{\partial x_0} + (1-\alpha_0)\frac{\partial p_{\mathrm{L2}}}{\partial x_0} - \alpha_0 B\frac{\partial p_{\mathrm{L2}}}{\partial x_0} = K_4, \tag{54}$$

$$\left[3(\gamma_{\mathrm{e}}-1)p_{\mathrm{G0}} - \frac{\Delta^2}{\Omega^2}\right]R_2 + p_{\mathrm{G0}}T_{\mathrm{G2}} - p_{\mathrm{L2}} = K_5, \tag{55}$$

$$\frac{\mathrm{D}T_{\mathrm{G2}}}{\mathrm{D}t_0} + 3(\kappa-1)\frac{\mathrm{D}R_2}{\mathrm{D}t_0} = K_6, \tag{56}$$

where the inhomogeneous terms K_i $(1 \le i \le 6)$ are explicitly presented in the Appendix. Consequently, (51)–(56) are combined into a single inhomogeneous equation,

$$\frac{\mathrm{D}^2 R_2}{\mathrm{D}t_0^2} - v_{\mathrm{p}}^2\frac{\partial^2 R_2}{\partial x_0^2} = K(f;t_1,x_1,\varphi_0), \tag{57}$$

where $f = f(t_1,x_1,\varphi_0)$ is the first order perturbation of the nondimensional bubble radius R_1 and K is given by

$$K = -\frac{1}{3}\frac{\mathrm{D}K_1}{\mathrm{D}t_0} + \frac{1}{3\alpha_0}\frac{\mathrm{D}K_2}{\mathrm{D}t_0} + \frac{u_0}{3\alpha_0(1-\alpha_0)}\frac{\partial K_2}{\partial x_0} + \frac{1-\alpha_0+\beta_1}{3(1-\alpha_0)\beta_1}\frac{\partial K_3}{\partial x_0} + \frac{1}{3\alpha_0(1-\alpha_0)}\frac{\partial K_4}{\partial x_0} + \frac{\beta_1+\alpha_0 B}{3\alpha_0\beta_1}\frac{\partial^2 K_5}{\partial x_0^2} - \frac{p_{\mathrm{G0}}[\alpha_0(1-\alpha_0)+\beta_1+\alpha_0 B(1-\alpha_0)]}{3\alpha_0\beta_1(1-\alpha_0)}\int\frac{\partial^2 K_6}{\partial {x_0}^2}\mathrm{d}t_0. \tag{58}$$

Based on the solvability condition for (57), $K=0$ is required.[31] From (24), the original independent variables x and t are restored

$$\frac{\partial f}{\partial t} + (u_0+v_{\mathrm{p}})\frac{\partial f}{\partial x} + \epsilon\left(\Pi_0\frac{\partial f}{\partial x} + \Pi_1 f\frac{\partial f}{\partial x} + \Pi_2\frac{\partial^2 f}{\partial x^2} + \Pi_3\frac{\partial^3 f}{\partial x^3} + \Pi_4 f\right) = 0. \tag{59}$$

Finally, we obtain the KdVB equation

$$\frac{\partial f}{\partial \tau} + \Pi_1 f\frac{\partial f}{\partial \xi} + \Pi_2\frac{\partial^2 f}{\partial \xi^2} + \Pi_3\frac{\partial^3 f}{\partial \xi^3} + \Pi_4 f = 0, \tag{60}$$

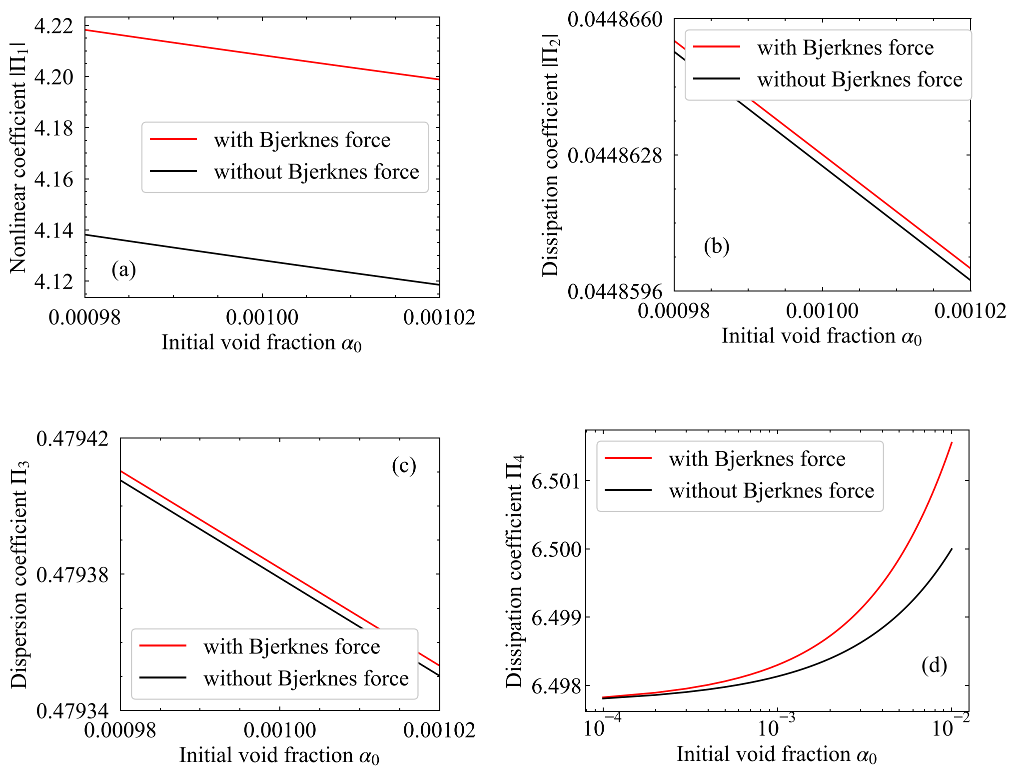

FIG. 2. The effect of Bjerknes forces on each coefficient: (a) Absolute value of nonlinearity $|\Pi_1|$, (b) dissipation owing to liquid compressibility $|\Pi_2|$ (see also Table II), (c) dispersion Π_3 (see also Table III), and (d) dissipation Π_4 as a function of α_0 for the case of $R_0^* = 500\,\mu$m, $\sqrt{\epsilon} = 0.15$, $p_{\mathrm{L0}}^* = 101\,325$ Pa, $\rho_{\mathrm{L0}}^* = 1000$ kg/m^3, $\sigma^* = 0.0728$ N/m, $c_{\mathrm{L0}}^* = 1500$ m/s, $\mu_{\mathrm{L}}^* = 10^{-3}$ Pa · s, $u_0 = 1$, and $v_{\mathrm{p}} = 1$.

TABLE II. Detailed value of the dissipation coefficient $|\Pi_2|$ in Fig. 2.

R_0^*	α_0	$\|\Pi_2\|\|_{B=0}$	$(\|\Pi_2\|\|_{B=1} - \|\Pi_2\|\|_{B=0})/\|\Pi_2\|\|_{B=0}$
5 mm	0.0001 (0.01%)	4.6×10^{-2}	6.0×10^{-6}
	0.001 (0.1%)	4.5×10^{-2}	6.0×10^{-4}
	0.01 (1%)	4.4×10^{-2}	5.7×10^{-2}
500 μm	0.0001 (0.01%)	4.5×10^{-2}	6.0×10^{-6}
	0.001 (0.1%)	4.5×10^{-2}	6.0×10^{-4}
	0.01 (1%)	4.4×10^{-2}	5.7×10^{-2}
50 μm	0.0001 (0.01%)	4.3×10^{-2}	6.0×10^{-6}
	0.001 (0.1%)	4.3×10^{-2}	6.0×10^{-4}
	0.01 (1%)	4.2×10^{-2}	5.8×10^{-2}

TABLE III. Detailed value of the dispersion coefficient Π_3 in Fig. 2.

R_0^*	α_0	$\Pi_3\|_{B=0}$	$(\Pi_3\|_{B=1} - \Pi_3\|_{B=0})/\Pi_3\|_{B=0}$
5 mm	0.0001 (0.01%)	4.9×10^{-1}	6.0×10^{-6}
	0.001 (0.1%)	4.9×10^{-1}	6.0×10^{-4}
	0.01 (1%)	4.8×10^{-1}	5.7×10^{-2}
500 μm	0.0001 (0.01%)	4.8×10^{-1}	6.0×10^{-6}
	0.001 (0.1%)	4.8×10^{-1}	6.0×10^{-4}
	0.01 (1%)	4.7×10^{-1}	5.7×10^{-2}
50 μm	0.0001 (0.01%)	4.4×10^{-1}	6.0×10^{-6}
	0.001 (0.1%)	4.4×10^{-1}	6.0×10^{-4}
	0.01 (1%)	4.3×10^{-1}	5.8×10^{-2}

using a variable transform

$$\tau = \epsilon t, \quad \xi = x - (u_0 + v_p + \epsilon\Pi_0)t, \tag{61}$$

where the constant coefficients are expressed as

$$\Pi_0 = \frac{1-\alpha_0}{6\alpha_0} V^2 v_p \left[3p_{G0}(\gamma_e - \kappa) - \frac{\Delta^2}{\Omega^2}\right], \tag{62}$$

$$\Pi_1 = \frac{1}{6}\left\{k_1 + \frac{u_0 - (1-\alpha_0)v_p}{\alpha_0(1-\alpha_0)v_p}k_2 + \frac{1-\alpha_0+\beta_1}{(1-\alpha_0)\beta_1 v_p}k_3 + \frac{k_4}{\alpha_0(1-\alpha_0)v_p} + \frac{\beta_1+\alpha_0 B}{\alpha_0\beta_1 v_p}k_5 + \frac{p_{G0}[\alpha_0(1-\alpha_0)+\beta_1+\alpha_0 B(1-\alpha_0)]}{\alpha_0\beta_1(1-\alpha_0)v_p^2}k_6\right\} < 0, \tag{63}$$

$$\begin{cases} k_1 = 6v_p(2-s_1) + 2s_2(3-s_1), \\ k_2 = -2\alpha_0 s_1 s_3, \\ \hat{k} = (\beta_1+\beta_2)s_1(s_2-s_3)v_p - \beta_1(s_2^2 - s_3^2) - Bs_1 s_4, \\ k_3 = p_{G0}s_1(3-s_5) + 6p_{G0}(s_5-2) + \hat{k}, \\ k_4 = -\alpha_0\hat{k} + \alpha_0 s_1 s_4 - 2(1-\alpha_0)s_3^2 - 2\alpha_0 s_1 s_3(v_p - u_0), \\ k_5 = -6p_{G0}(3\kappa - \gamma_e - 1) - \dfrac{2\Delta^2}{\Omega^2} - \dfrac{1}{2}(s_2-s_3)^2, \\ k_6 = -3v_p(3\kappa^2 - 5\kappa + 2), \end{cases} \tag{64}$$

$$\Pi_2 = \frac{\beta_1+\alpha_0 B}{6\alpha_0\beta_1}V\Delta\left[3p_{G0}(\gamma_e-\kappa) - \frac{\Delta^2}{\Omega^2}\right] < 0, \tag{65}$$

$$\Pi_3 = \frac{\beta_1+\alpha_0 B}{6\alpha_0\beta_1}\Delta^2 v_p > 0, \tag{66}$$

$$\Pi_4 = \Pi_{4buo} + \Pi_{4gr} + \Pi_{4dr} + \Pi_{4th} > 0, \tag{67}$$

$$\Pi_{4buo} = \frac{s_1 g}{6\beta_1 v_p} > 0, \tag{68}$$

$$\Pi_{4gr} = \frac{s_1 g}{6(1-\alpha_0)v_p} > 0, \tag{69}$$

$$\Pi_{4dr} = \frac{A\mu_L}{32 v_p \beta_1 \Delta^2}(s_3 - s_2) > 0, \tag{70}$$

$$\Pi_{4th} = \frac{p_{G0}[\alpha_0(1-\alpha_0)+\beta_1+\alpha_0 B(1-\alpha_0)]}{2\alpha_0\beta_1(1-\alpha_0)v_p^2}(\kappa-1)\zeta_{STM1} > 0, \tag{71}$$

where Π_0 is the advection coefficient, Π_1 is the nonlinear coefficient, Π_2 and Π_4 are the dissipation coefficients, and Π_3 is the dispersion coefficient. Furthermore, Π_2, Π_{4buo}, Π_{4gr}, Π_{4dr}, and Π_{4th} are the dissipation coefficients owing to acoustic radiation (i.e., liquid compressibility), buoyancy, gravity, drag, and thermal conduction, respectively.

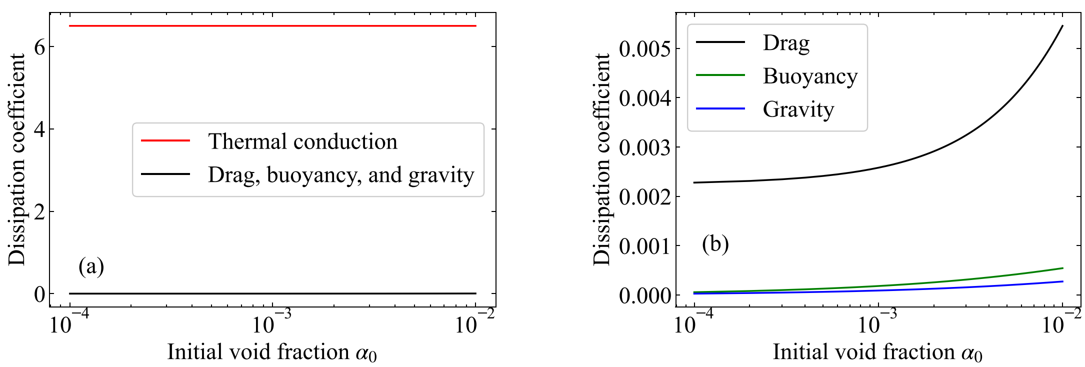

FIG. 3. Comparison of the dissipation coefficients: (a) The red and black curves represent the coefficient owing to thermal conduction and the sum of drag, buoyancy, and gravity; (b) the black, green, and blue curves represent the coefficient owing to drag, buoyancy, and gravity, respectively (see also Table IV). The condition is the same as that in Fig. 2.

TABLE IV. Detailed value of comparison of drag, buoyancy, and gravity in Fig. 3.

R_0^*	α_0	Π_{4dr}	Π_{4buo}	Π_{4gr}
5 mm	0.0001 (0.01%)	7.4×10^{-5}	5.9×10^{-4}	2.9×10^{-4}
	0.001 (0.1%)	1.0×10^{-4}	1.9×10^{-3}	9.3×10^{-4}
	0.01 (1%)	4.0×10^{-4}	5.5×10^{-3}	2.8×10^{-3}
1 mm	0.0001 (0.01%)	8.1×10^{-4}	1.2×10^{-4}	5.9×10^{-5}
	0.001 (0.1%)	9.6×10^{-4}	3.7×10^{-4}	1.8×10^{-4}
	0.01 (1%)	2.4×10^{-3}	1.1×10^{-3}	5.5×10^{-4}
500 μm	0.0001 (0.01%)	2.3×10^{-3}	5.9×10^{-5}	2.9×10^{-5}
	0.001 (0.1%)	2.6×10^{-3}	1.8×10^{-4}	9.2×10^{-5}
	0.01 (1%)	5.5×10^{-3}	5.4×10^{-4}	2.8×10^{-4}
50 μm	0.0001 (0.01%)	7.1×10^{-2}	5.7×10^{-6}	2.8×10^{-6}
	0.001 (0.1%)	7.4×10^{-2}	1.8×10^{-5}	8.9×10^{-6}
	0.01 (1%)	1.0×10^{-1}	5.3×10^{-5}	2.7×10^{-5}
10 μm	0.0001 (0.01%)	7.1×10^{-1}	1.0×10^{-6}	5.2×10^{-7}
	0.001 (0.1%)	7.3×10^{-1}	3.2×10^{-6}	1.6×10^{-6}
	0.01 (1%)	8.5×10^{-1}	9.6×10^{-6}	4.9×10^{-6}

In this way, the present theory could divide the total attenuation of waves into independent attenuation components due to various forces.

C. Discussion

The relationship between the Bjerknes force and coefficients is shown in Fig. 2 and Tables II and III. The absolute values of nonlinear, dissipation, and dispersion coefficients increased owing to the Bjerknes force. In particular, the effect of the Bjerknes force on Π_4 is significant. A comparison of the dissipation coefficients Π_4 is shown in Fig. 3 and Table IV. The dissipation effect of thermal conduction was the largest, followed by those of drag, buoyancy, and gravity. It should be noted that, as this result depends on the temperature-gradient model,[82] the influence of thermal conduction on the waves may be overestimated.

The dissipation term owing to acoustic radiation (i.e., $\Pi_2 \partial^2 f/\partial \xi^2$) has a different mechanism from that owing to drag, gravity, buoyancy, and thermal conduction (i.e., $\Pi_4 f$) with respect to the unknown variable. We then conducted a numerical analysis using a spectral method based on the split-step Fourier method used in previous studies[59,63,84] to compare each dissipation effect. Our previous study[63] considered three dissipation effects and indicated that the dissipation effect of the thermal conduction was the largest, followed by those of acoustic radiation and drag force obtained from the numerical analysis. Figure 4 illustrates the temporal evolution of the numerical solutions to the KdVB equation (60). The black, blue, and red curves represent waveforms with only acoustic radiation, with drag, gravity, and buoyancy forces and with only thermal conduction, respectively. The initial waveform of the solution is assumed to be a cosine wave. The dissipation effect of thermal conduction was the largest, followed by those of acoustic radiation, drag, buoyancy, and gravity. This order was effective in the range from $R_0^* = 50\,\mu$m to 1 mm. As shown in Table IV, the larger the initial bubble radius R_0^* the smaller the damping effect of drag Π_{4dr}. At $R_0^* = 5$ mm, the damping effect of drag was smaller than that of gravity. At $R_0^* = 10\,\mu$m, the damping effect of drag was larger than that of acoustic radiation.

IV. CONCLUSIONS

Many previous theoretical studies (e.g., Refs. 32–36) have not clarified the relationship between the forces acting on bubbles and waves in bubbly flows. Although the validity of ignoring forces acting on the bubble has not been demonstrated, previous theoretical studies on nonlinear pressure waves in bubbly flows did not incorporate these forces. In this study, we theoretically examined the weakly nonlinear propagation of plane (one-dimensional) pressure progressive waves in water flows uniformly containing many spherical bubbles, particularly focusing on the effects of gravity, buoyancy, and (primary) Bjerknes forces acting on bubbles. Using the singular perturbation method (multiple scales analysis), the KdVB equation describing weakly

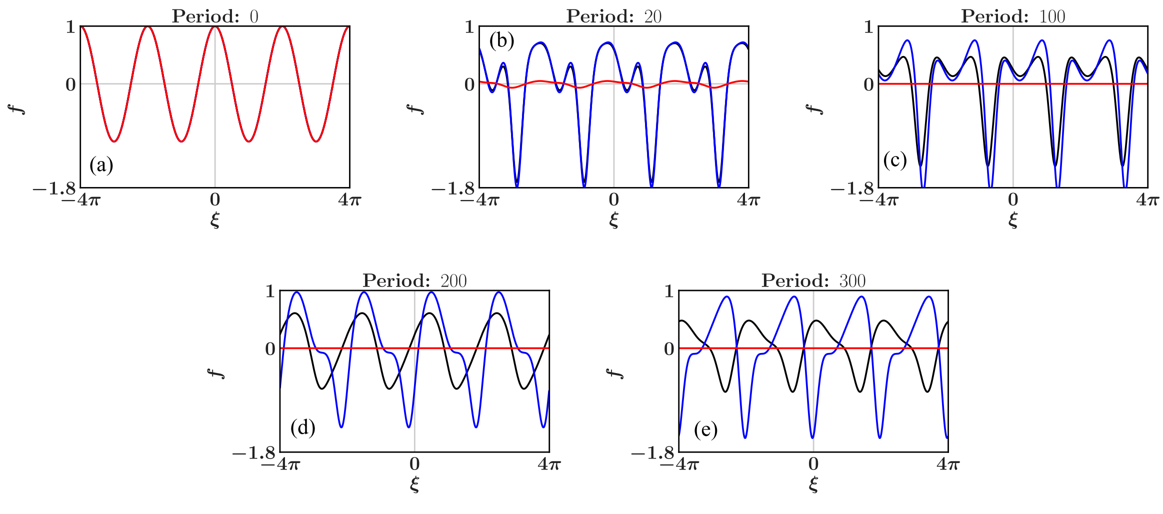

FIG. 4. Example of the numerical solution of (60) for $\alpha_0 = 0.001$ and $R_0^* = 500\,\mu$m. Horizontal axis is the nondimensional space coordinate ξ. The vertical axis is the first order perturbation of the nondimensional bubble radius f. The period is (a) 0, (b) 20, (c) 100, (d) 200, and (e) 300. The black, blue, and red curves represent the waveforms with only the acoustic radiation, with the drag, gravity, and buoyancy force, and with only the thermal conduction, respectively. The condition is the same as that in Fig. 2. Other conditions are grid steps 1024, the duration of the numerical integration of time 0.001, and the size of computational domain 8π.

nonlinear propagation of long waves with a low frequency was derived. The following findings were obtained:

(i) The Bjerknes force acting on the bubbles contributed to the nonlinearity, dissipation, and dispersion of waves and increased the three effects.
(ii) The drag, gravity, and buoyancy forces acting on the bubbles contributed to dissipation and increased the value of the dissipation coefficients.
(iii) In the range from $R_0^* = 50\,\mu$m to 1 mm, the dissipation effect decreased in the order: thermal conduction, acoustic radiation, drag, buoyancy, and gravity.

This study revealed that the attenuation of waves owing to the forces acting on gas bubbles is quantitatively small. This is the first study to demonstrate the validity of ignoring forces for pressure wave propagation in bubbly flows.

A lift could not be introduced here because this study considered only the one-dimensional case. The effect of forces such as lift[44–46] and buoyancy force on waves will be investigated in future research in the framework of multidimensional problem.

ACKNOWLEDGMENTS

This work was partly carried out with the aid of JSPS KAKENHI (No. 22K03898), the JKA and its promotion funds from KEIRIN RACE, and the Komiya Research Grant from the Turbomachinery Society of Japan. This work was partly based on results obtained from a project subsidized by the New Energy and Industrial Technology Development Organization (NEDO) (No. JPNP20004). This work was partly supported by the Top Runners in Strategy of Transborder Advanced Researches (TRiSTAR) program conducted as the Strategic Professional Development Program for Young Researchers by the MEXT. We would like to thank four referees for their valuable comments and Editage (www.editage.com) for English language editing.

AUTHOR DECLARATIONS

Conflict of Interest

The authors have no conflicts to disclose.

Author Contributions

Shuya Arai and Tetsuya Kanagawa contributed equally to this work.

Shuya Arai: Formal analysis (equal); Investigation (equal); Methodology (equal); Software (lead); Validation (equal); Visualization (lead); Writing – original draft (equal); Writing – review & editing (equal). **Tetsuya Kanagawa:** Conceptualization (lead); Formal analysis (equal); Funding acquisition (lead); Investigation (equal); Methodology (equal); Project administration (lead); Software (supporting); Supervision (lead); Validation (equal); Visualization (supporting); Writing – original draft (equal); Writing – review & editing (equal).

DATA AVAILABILITY

The data that support the findings of this study are available from the corresponding author upon reasonable request.

APPENDIX: INHOMOGENEOUS TERMS

The inhomogeneous terms K_i $(1 \le i \le 6)$ in (51)–(56) are given by

$$K_1 = -\frac{\partial u_{G1}}{\partial x_1} + \frac{D}{Dt_1}(3R_1 - \alpha_1) + 3\frac{D}{Dt_0}[R_1(\alpha_1 - 2R_1)] + \frac{\partial}{\partial x_0}[u_{G1}(3R_1 - \alpha_1)], \tag{A1}$$

$$K_2 = (1-\alpha_0)\frac{\partial u_{L1}}{\partial x_1} - \alpha_0\frac{D\alpha_1}{Dt_1} - \alpha_0\frac{\partial}{\partial x_0}(\alpha_1 u_{L1}) + (1-\alpha_0)\frac{D\rho_{L1}}{Dt_0}, \tag{A2}$$

$$K_3 = p_{G0}\frac{\partial}{\partial x_1}(3R_1 - T_{G1}) + p_{G0}\alpha_1\frac{\partial}{\partial x_0}(3R_1 - T_{G1}) + 3p_{G0}\frac{\partial}{\partial x_0}[R_1(T_{G1} - 2R_1)] + K_F, \tag{A3}$$

$$\begin{aligned} K_4 =& \frac{D}{Dt_1}[u_0\alpha_0\alpha_1 - (1-\alpha_0)u_{L1}] - (1-\alpha_0)\frac{\partial}{\partial x_1}(p_{L1} + u_0 u_{L1}) \\ &+ \alpha_0\frac{D}{Dt_0}(\alpha_1 u_{L1}) + u_0\alpha_0\frac{\partial}{\partial x_0}(\alpha_1 u_{L1}) - (1-\alpha_0)\frac{\partial u_{L1}^2}{\partial x_0} \\ &+ \alpha_0\alpha_1\frac{\partial p_{L1}}{\partial x_0} - \alpha_0 K_F - (1-\alpha_0)u_0\frac{D\rho_{L1}}{Dt_0} \\ &- \alpha_0\left\{\left[3(\gamma_e - 1)p_{G0} - \frac{\Delta^2}{\Omega^2}\right]R_1 + p_{G0}T_{G1} - p_{L1}\right\}\frac{\partial \alpha_1}{\partial x_0} + g\alpha_0\alpha_1, \end{aligned} \tag{A4}$$

$$K_5 = \Delta^2\frac{D^2 R_1}{Dt_0^2} - V\Delta\frac{D p_{L1}}{Dt_0} + 3p_{G0}R_1T_{G1} - \left[3(2-\gamma_e)p_{G0} + \frac{\Delta^2}{\Omega^2}\right]R_1^2 - \frac{1}{4}(u_{G1} - u_{L1})^2, \tag{A5}$$

$$K_6 = -3\frac{D}{Dt_0}\left[(\kappa - 1)T_{G1}R_1 + \frac{1}{2}(\kappa - 1)(3\kappa - 4)R_1^2\right] - \zeta_{STM1}T_{G1}, \tag{A6}$$

where

$$\frac{D}{Dt_1} = \frac{\partial}{\partial t_1} + u_0\frac{\partial}{\partial x_1}, \tag{A7}$$

$$\begin{aligned} K_F =& -\beta_1\frac{D}{Dt_1}(u_{G1} - u_{L1}) - \beta_1\alpha_1\frac{D}{Dt_0}(u_{G1} - u_{L1}) \\ &- \beta_1\left(u_{G1}\frac{\partial u_{G1}}{\partial x_0} - u_{L1}\frac{\partial u_{L1}}{\partial x_0}\right) - \beta_2(u_{G1} - u_{L1})\frac{D\alpha_1}{Dt_0} \\ &- \frac{3A\mu_L}{16\Delta^2}(u_{G1} - u_{L1}) + \alpha_1 g - B\left(\frac{\partial p_{L1}}{\partial x_1} + \alpha_1\frac{\partial p_{L1}}{\partial x_0}\right). \end{aligned} \tag{A8}$$

REFERENCES

[1]E. Goncalves, Y. Hoarau, and D. Zeidan, "Simulation of shock-induced bubble collapse using a four-equation model," Shock Waves **29**, 221–234 (2019).
[2]D. Zeidan, M. Pandey, and S. Govekar, "Interaction of shock and discontinuity waves at the stellar surfaces," Phys. Fluids **34**, 066111 (2022).
[3]X. Zhao, Z. Wang, X. Bai, H. Cheng, and B. Ji, "Unsteady cavitation dynamics and pressure statistical analysis of a hydrofoil using the compressible cavitation model," Phys. Fluids **35**, 103307 (2023).
[4]M. K. Li, S. P. Wang, S. Zhang, and H. Sagar, "Experimental study of underwater explosions below a free surface: Bubble dynamics and pressure wave emission," Phys. Fluids **35**, 083313 (2023).

[5]J. J. Schoppink, K. Mohan, M. A. Q. Santiago, G. McKinley, D. F. Rivas, and A. K. Dickerson, "Cavitation-induced microjets tuned by channels with alternating wettability patterns," Phys. Fluids **35**, 032017 (2023).
[6]P. Kangude and A. Srivastava, "Experiments to understand bubble base evaporation mechanisms and heat transfer on nano-coated surfaces of varying wettability under nucleate pool boiling regime," Int. J. Multiph. Flow **152**, 104098 (2022).
[7]D. Raciti, P. Brocca, A. Raudino, and M. Corti, "Interferometric detection of hydrodynamic bubble–bubble interactions," J. Fluid Mech **942**, R1 (2022).
[8]T. Ma, H. Hessenkemper, D. Lucas, and A. D. Bragg, "Effects of surfactants on bubble-induced turbulence," J. Fluid Mech. **970**, A13 (2023).
[9]L. Wang, P. Wang, K. Wu, H. Wang, B. Huang, and D. Wu, "Experiment investigation of the tip vortex cavitation around a pitching hydrofoil," Phys. Fluids **35**, 103313 (2023).
[10]H. A. Kamali and M. Pasandidehfard, "Investigating the interaction parameters on ventilation supercavitation phenomena: Experimental and numerical analysis with machine learning interpretation," Phys. Fluids **35**, 113325 (2023).
[11]Q. Li, R. Zhang, H. Xu, and H. Ye, "Experimental investigation on diffusion and fountain behavior of bubble plumes in quiescent water," Phys. Fluids **35**, 123314 (2023).
[12]V. T. Nguyen, T. H. Phan, and W. G. Park, "Modeling of shock wave produced by collapse of cavitation bubble using a fully conservative multiphase model," Phys. Fluids **35**, 116102 (2023).
[13]D. Igra and O. Igra, "Numerical investigation of the interaction between a converging shock wave and an offset cylindrical bubble containing different gases," Phys. Fluids **35**, 076115 (2023).
[14]J. Wang, S. Li, J. Gu, and A. M. Zhang, "Particle propulsion from attached acoustic cavitation bubble under strong ultrasonic wave excitation," Phys. Fluids **35**, 042009 (2023).
[15]F. Tan, T. Wu, L. Gao, F. Li, Z. He, Y. Li, and J. Li, "Numerical investigation of bubble behavior and multiphase flow in ladle using purging plug with inclined slit designs," Int. J. Multiph. Flow **172**, 104709 (2024).
[16]K. Roy and S. Paruya, "On the mechanics of thermal collapse of a vapor bubble translating in an isothermal subcooled liquid," Int. J. Multiph. Flow **171**, 104691 (2024).
[17]A. Yu, W. Feng, and Q. Tang, "Numerical study on the pulsating energy evolution in the cavitating flow around a mini Cascade," Phys. Fluids **34**, 123308 (2022).
[18]X. Luo, T. Chen, W. Xiao, X. L. Yao, and J. L. Liu, "The dynamics of a bubble in the internal fluid flow of a pipeline," Phys. Fluids **34**, 117103 (2022).
[19]Y. Liu, W. Wang, G. Yang, H. Nemati, and X. Chu, "The interfacial modes and modal causality in a dispersed bubbly turbulent flow," Phys. Fluids **35**, 083309 (2023).
[20]Q. Wang, B. Wang, C. Wan, H. Zhang, and Y. Liu, "Modeling the distribution characteristics of vapor bubbles in cavitating flows," Phys. Fluids **35**, 123316 (2023).
[21]A. M. R. A. Gaheeshi, F. L. Rashid, and H. I. Mohammed, "Dynamics of single bubble ascension in stagnant liquid: An investigation into multiphase flow effects on hydrodynamic characteristics using computational simulation," Phys. Fluids **35**, 123303 (2023).
[22]A. Alavi and E. Roohi, "Large eddy simulations of cavitation around a pitching–plunging hydrofoil," Phys. Fluids **35**, 125102 (2023).
[23]J. Zhang, X. Wang, C. Yang, J. Tang, and Z. Huang, "Cavitation flow and noise reduction design of bionic hydrofoil based on orthogonal optimization," Phys. Fluids **35**, 115132 (2023).
[24]H. Yan, H. Gong, Z. Huang, P. Zhou, and L. Liu, "Euler–Euler modeling of reactive bubbly flow in a bubble column," Phys. Fluids **34**, 053306 (2022).
[25]A. Saha and A. K. Das, "Bubble dynamics in concentric multi-orifice column under normal and reduced gravity," Phys. Fluids **34**, 042113 (2022).
[26]Y. Zang, "Radial and translational motions of a gas bubble in a Gaussian standing wave field," Ultrason. Sonochem. **101**, 106712 (2023).
[27]A. Shukla and S. Datta, "Asymptotic theory for damped dynamics of gas-filled bubbles," Appl. Math. Modell. **125**, 499–513 (2024).
[28]D. A. Gubaidullin and Y. V. Fedorov, "Acoustics of a viscoelastic medium with encapsulated bubbles," J. Hydrodyn. **33**, 55–62 (2021).
[29]Y. D. Chou, W. S. Hwang, M. Solovchuk, P. G. Siddheshwar, T. W. H. Sheu, and S. Chakraborty, "Weakly nonlinear stability analysis of salt-finger convection in a longitudinally infinite cavity," Phys. Fluids **34**, 011908 (2022).
[30]G. B. Whitham, *Linear and Nonlinear Waves* (Wiley, New York, 1974).
[31]A. Jeffrey and T. Kawahara, *Asymptotic Methods in Nonlinear Wave Theory* (Pitman, London, 1982).
[32]R. S. Johnson, "A non-linear equation incorporating damping and dispersion," J. Fluid Mech. **42**, 49–60 (1970).
[33]L. van Wijngaarden, "On the equations of motion for mixtures of liquid and gas bubbles," J. Fluid Mech. **33**, 465–474 (1968).
[34]L. van Wijngaarden, "One-dimensional flow of liquids containing small gas bubbles," Annu. Rev. Fluid Mech. **4**, 369–396 (1972).
[35]R. I. Nigmatulin, *Dynamics of Multiphase Media* (Hemisphere, New York, 1991).
[36]V. V. Kuznetsov, V. E. Nakoryakov, B. G. Pokusaev, and I. R. Shreiber, "Propagation of perturbations in a gas-liquid mixture," J. Fluid Mech. **85**, 85–96 (1978).
[37]A. Tomiyama, I. Kataoka, I. Zun, and T. Sakaguchi, "Drag coefficients of single bubbles under normal and microgravity conditions," JSME Int. J., Ser. B **41**, 472–479 (1998).
[38]M. Ishii and T. C. Chawla, "Local drag laws in dispersed two-phase flow," Report Nos. NUREG/CR-1230 and ANL-79-105 (Argonne National Laboratory, 1979).
[39]J. Magnaudet and D. Legendre, "The viscous drag force on a spherical bubble with a time-dependent radius," Phys. Fluids **10**, 550–554 (1998).
[40]C. E. Brennen and E. Christopher, *Cavitation and Bubble Dynamics* (Cambridge University Press, 2014).
[41]G. Yang, H. Zhang, J. Luo, and T. Wang, "Drag force of bubble swarms and numerical simulations of a bubble column with a CFD-PBM coupled model," Chem. Eng. Sci. **192**, 714–724 (2018).
[42]R. Mettin and A. A. Doinikov, "Translational instability of a spherical bubble in a standing ultrasound wave," Appl. Acoust. **70**, 1330–1339 (2009).
[43]P. Shi, V. Tholan, A. E. Sommer, S. Heitkam, K. Eckert, K. Galvin, and R. Rzehak, "Forces on a nearly spherical bubble rising in an inclined channel flow," Int. J. Multiph. Flow **169**, 104620 (2023).
[44]P. G. Saffman, "The lift on a small sphere in a slow shear flow," J. Fluid Mech. **22**, 385–400 (1965).
[45]D. Legendre and J. Magnaudet, "The lift force on a spherical bubble in a viscous linear shear flow," J. Fluid Mech. **368**, 81–126 (1998).
[46]D. Lucas, E. Krepper, and H. M. Prasser, "Use of models for lift, wall and turbulent dispersion forces acting on bubbles for poly-disperse flows," Chem. Eng. Sci. **62**, 4146–4157 (2007).
[47]O. E. Azpitarte and G. C. Buscaglia, "Analytical and numerical evaluation of two-fluid model solutions for laminar fully developed bubbly two-phase flows," Chem. Eng. Sci. **58**, 3765–3776 (2003).
[48]A. Sokolichin, G. Eigenberger, and A. Lapin, "Simulation of buoyancy driven bubbly flow: Established simplifications and open questions," AIChE J. **50**, 24–45 (2004).
[49]Z. Wang, H. Cheng, R. E. Bensow, X. Peng, and B. Ji, "Numerical assessment of cavitation erosion risk on the Delft twisted hydrofoil using a hybrid Eulerian-Lagrangian strategy," Int. J. Mech. Sci. **259**, 108618 (2023).
[50]T. Yano, R. Egashira, and S. Fujikawa, "Linear analysis of dispersive waves in bubbly flows based on averaged equations," J. Phys. Soc. Jpn. **75**, 104401 (2006).
[51]V. F. K. Bjerknes, *Fields of Force* (Columbia University Press, New York, 1906).
[52]L. A. Crum, "Bjerknes forces on bubbles in a stationary sound field," J. Acoust. Soc. Am. **57**, 1363–1370 (1975).
[53]T. G. Leighton, A. J. Walton, and M. J. W. Pickworth, "Primary Bjerknes forces," Eur. J. Phys. **11**, 47–50 (1990).
[54]T. J. Matula, S. M. Cordry, R. A. Roy, and L. A. Crum, "Bjerknes force and bubble levitation under single-bubble sonoluminescence conditions," J. Acoust. Soc. Am. **102**, 1522–1527 (1997).
[55]O. Louisnard, "A simple model of ultrasound propagation in a cavitating liquid. Part II: Primary Bjerknes force and bubble structures," Ultrason. Sonochem. **19**, 66–76 (2012).
[56]V. D. Kubenko and I. V. Yanchevs'kyi, "Diffraction field and radiation force for a liquid bubble in a dissimilar fluid in an infinite cylindrical cavity," Int. Appl. Mech. **59**, 257–269 (2023).
[57]J. Janiak, Y. Li, Y. Ferry, A. A. Doinikov, and D. Ahmed, "Acoustic microbubble propulsion, train-like assembly and cargo transport," Nat. Commun. **14**, 4705 (2023).

[58]S. Lesnik, A. Aghelmaleki, R. Mettin, and G. Brenner, "Modeling acoustic cavitation with inhomogeneous polydisperse bubble population on a large scale," Ultrason. Sonochem. **89**, 106060 (2022).
[59]T. Yatabe, T. Kanagawa, and T. Ayukai, "Theoretical elucidation of effect of drag force and translation of bubble on weakly nonlinear pressure waves in bubbly flows," Phys. Fluids **33**, 033315 (2021).
[60]T. Yatabe, T. Kanagawa, and T. Ayukai, "Numerical study on weakly nonlinear evolution of pressure waves in water flows containing many translational bubbles acting a drag force," Jpn. J. Multiphase Flow **35**, 356–364 (2021).
[61]T. Kanagawa, T. Ayukai, T. Maeda, and T. Yatabe, "Effect of drag force and translation of bubbles on nonlinear pressure waves with a short wavelength in bubbly flows," Phys. Fluids **33**, 053314 (2021).
[62]S. Arai, T. Kanagawa, T. Ayukai, and T. Yatabe, "Nonlinear and dissipation effects of pressure waves in water flows containing translational bubbles with a drag force," J. Phys.: Conf. Ser. **2217**, 012021 (2022).
[63]S. Arai, T. Kanagawa, and T. Ayukai, "Nonlinear pressure waves in bubbly flows with drag force: Theoretical and numerical comparison of acoustic and thermal and drag force dissipations," J. Phys. Soc. Jpn. **91**, 043401 (2022).
[64]A. J. Sojahrood, H. Haghi, R. Karshafian, and M. C. Kolios, "Nonlinear dynamics and bifurcation structure of ultrasonically excited lipid coated microbubbles," Ultrason. Sonochem. **72**, 105405 (2021).
[65]A. J. Sojahrood, Q. Li, H. Haghi, R. Karshafian, T. M. Porter, and M. C. Kolios, "Probing the pressure dependence of sound speed and attenuation in bubbly media: Experimental observations, a theoretical model and numerical calculations," Ultrason. Sonochem. **95**, 106319 (2023).
[66]H. U. Rehman, M. Shuaib, E. A. A. Ismail, and S. Li, "Enhancing medical ultrasound imaging through fractional mathematical modeling of ultrasound bubble dynamics," Ultrason. Sonochem. **100**, 106603 (2023).
[67]Y. Wang, D. Chen, and P. Wu, "Multi-bubble scattering acoustic fields in viscoelastic tissues under dual-frequency ultrasound," Ultrason. Sonochem. **99**, 106585 (2023).
[68]A. Gnanaskandan, C. T. Hsiao, and G. Chahine, "Modeling of microbubble-enhanced high-intensity focused ultrasound," Ultrasound Med. Biol. **45**, 1743–1761 (2019).
[69]Y. Fan, H. Li, J. Zhu, and W. Du, "A simple model of bubble cluster dynamics in an acoustic field," Ultrason. Sonochem. **64**, 104790 (2020).
[70]R. Mettin, I. Akhatov, U. Parlitz, C. D. Ohl, and W. Lauterborn, "Bjerknes forces between small cavitation bubbles in a strong acoustic field," Phys. Rev. E **56**, 2924–2931 (1997).
[71]A. A. Doinikov, "Effects of the second harmonic on the secondary Bjerknes force," Phys. Rev. E **59**, 3016–3021 (1999).
[72]K. Yoshida, T. Fujikawa, and Y. Watanabe, "Experimental investigation on reversal of secondary Bjerknes force between two bubbles in ultrasonic standing wave," J. Acoust. Soc. Am. **130**, 135–144 (2011).
[73]J. Jiao, Y. He, S. E. Kentish, M. Ashokkumar, R. Manasseh, and J. Lee, "Experimental and theoretical analysis of secondary Bjerknes forces between two bubbles in a standing wave," Ultrasonics **58**, 35–42 (2015).
[74]K. Feng, X. Li, A. Huang, M. Wan, and Y. Zong, "Effect of tissue viscoelasticity and adjacent phase-changed microbubbles on vaporization process and direct growth threshold of nanodroplet in an ultrasonic field," Ultrason. Sonochem. **101**, 106665 (2023).
[75]T. Ayukai and T. Kanagawa, "Derivation and stability analysis of two-fluid model equations for bubbly flow with bubble oscillations and thermal damping," Int. J. Multiph. Flow **165**, 104456 (2023).
[76]R. Egashira, T. Yano, and S. Fujikawa, "Linear wave propagation of fast and slow modes in mixtures of liquid and gas bubbles," Fluid Dyn. Res. **34**, 317–334 (2004).
[77]J. B. Keller and I. I. Kolodner, "Damping of underwater explosion bubble oscillations," J. Appl. Phys **27**, 1152–1161 (1956).
[78]A. Biesheuvel and L. van Wijngaarden, "Two-phase flow equations for a dilute dispersion of gas bubbles in liquid," J. Fluid Mech. **148**, 301–318 (1984).
[79]M. Kameda and Y. Matsumoto, "Shock waves in a liquid containing small gas bubbles," Phys. Fluids **8**, 322–335 (1996).
[80]K. Klapcsik and F. Hegedűs, "Numerical investigation of the translational motion of bubbles: The comparison of capabilities of the time-resolved and the time-averaged methods," Ultrason. Sonochem. **92**, 106253 (2023).
[81]A. Prosperetti, "The thermal behaviour of oscillating gas bubbles," J. Fluid Mech. **222**, 587–616 (1991).
[82]K. Sugiyama, S. Takagi, and Y. Matsumoto, "A new reduced-order model for the thermal damping effect on radial motion of a bubble (1st report, perturbation analysis)," Trans. Jpn. Soc. Mech. Eng., Ser. B **71**, 1011–1019 (2005).
[83]R. Clift and J. R. Grace, *Bubbles, Drops, and Particles* (Academic Press, 1978).
[84]T. Ayukai and T. Kanagawa, "Numerical study on nonlinear evolution of pressure waves in bubbly liquids: Effective range of initial void fraction," Proc. Mtgs. Acoust. **39**, 045009 (2019).